Electrospray propelled by ionic wind in a bipolar system for direct delivery of charge reduced nanoparticles

Van T. Dau[1,5*], Trung-Hieu Vu[1], Canh-Dung Tran[2], Thanh Viet Nguyen[3], Tuan-Khoa Nguyen[3], Toan Dinh[2], Hoang-Phuong Phan[3], Shimizu Kazunori[4], Nam-Trung Nguyen[3] and Dzung V. Dao[1,3]

[1]*School of Engineering and Built Environment, Griffith University, AUSTRALIA*

[2]*School of Mechanical and Electrical Engineering, University of Southern Queensland, AUSTRALIA*

[3]*Queensland Micro and Nanotechnology Centre, Griffith University, AUSTRALIA*

[4]*Institute for Advanced Research, Nagoya University, JAPAN*

[5]*Centre of Catalysis and Clean Energy, Griffith University, AUSTRALIA*

*email: v.dau@griffith.edu.au

Abstract: We present a conceptual design to generate and deliver nanoparticles in one unique system based on electrohydrodynamic atomization (EHDA) without the restriction of the collector. The present EHDA bipolar configuration consists of a capillary nozzle and a pin, both act as emitters and also the reference electrodes of each other. Under an applied voltage, the capillary nozzle sprays droplets while the pin generates ion wind via corona discharge. The interaction with counter ions by the corona discharge, droplets' charge is significantly reduced and then propelled away from the electrodes by the momentum of ion winds accumulated from corona discharges. Thus, the present technique can yield promising applications in effective respiratory delivery of nanomedicine.

Inhalation of particulate therapeutics through oral or nasal route represents a noninvasive, self-administration approach for the delivery to local respiratory systems as well as throughout the human body [1,2]. Compared with traditional therapeutics such as oral and parenteral drug deliveries, pulmonary drug delivery via inhalation offers significant advantages because digestion degradation can be avoided, allowing a high efficacy-to-safety ratio of therapeutic. Monodisperse 1–5 µm bronchodilator particles are optimal for drug delivery efficacy. However, recent experimental results pointed out that the range of optimal aerosol particle sizes might be much smaller than the currently assumed and covers a range only from 0.5–2.8 µm [3,4] which is a technique challenge.

Electrohydrodynamic atomization (EHDA), also named as electrospray (ES), is a simple but versatile technique with a unique capability of efficiently generating micro/nanoscale droplets. EHDA has emerged as a potential tool for drug delivery and discovery research [5,6] and attracts researchers to respiratory treatment, including the generation and delivery of micro/nanoparticles as carriers for nanomedicine [7–9]. Electrospray of liquids is generated on a liquid surface when it flows through a capillary in the electric field of a high voltage [10]. The basic set-up for electrospray includes (i) a nozzle being connected to a high voltage source and supplied with a liquid to be atomized into micro/nano particles and (ii) a grounded conducting plate which is usually installed in front of the nozzle to collect the particles. The electric field induces a radial electrostatic pressure on the liquid surface at the output, which is equilibrated by the capillary pressure, yielding a conical shape of liquid, called as Taylor cone, at the capillary output. A liquid filament is then ejected from the cone apex and broken into the mist of uniform droplets. Owing to be highly charged, particles/droplets can be efficiently collected by chips connected to either the electrical ground or an opposite potential. This however limits the usability of ES in a delivery procedure which includes two steps: the particle generation is then followed by the particle delivery via inhalation using a nebulizer, dry powder inhaler, pressurized metered dose inhaler or soft-mist inhalers [7].

For drug delivery by inhalation, the discharge of EHDA sprayed droplets/particles is an essential requirement as it decreases the electrostatic force on particles when they move through the inter-electrode region [11]. To achieve that, a counter ion source was required and installed in front of the spraying nozzle. Particles/droplets will be discharged when they move through a cloud of counter ions which is generated by a grounded sharp pin electrode of an additional system, allowing the particles be conveyed out of the effect of reference electrode by an external air flow [12,13]. More details can be found in [14–19]. This approach has been expanded to biologically active nano-aerosol neutralised by a cloud of oppositely charged ions from a volatile solvent [20] or oppositely charged double head electrosprays [21].

Alternatively, several alternating current (ac) EHDA approaches have been reported with significant physical and mechanistic differences. The performance of ac EHDA is qualitatively shown to be frequency dependent. For the high frequency case (i.e., from 10 kHz - 10 MHz), micron-sized particles are intermittently generated with resonating meniscus rather than continuously ejected from a sharp Taylor cone like dc counterpart. The resonant frequency of meniscus vibration and the drop ejection were attributed to the capillary-inertia vibration time and the electric stress at the drop tip, respectively. The primarily characteristic of stable cone-jet mode in dc electrosprays was not observable in high frequency ac spray[22,23], or appeared at much smaller value (~12.6˚)[24]. The droplets generated by ac EHDA have coarser size distribution, their charges are much less than that of droplets generated from a dc Taylor cone and depend on the entrainment of the low mobility ions[25]. At lower frequency (1kHz-4kHz), pulsating cone jet can be found via choked jet or oscillating cone regime[26]. As the frequency further reduces (~100Hz), the sprayed particles are self-neutralised via matching their momentum with reversing electric field[27]

The present work presents a dc used EHDA bipolar system scheme using , which integrates both particle generation and delivery in a single device. We employ two electrodes with opposite polarities to generate charged particles/droplets from a direct current power source. Notably, both electrodes serve as emitters and also the reference electrode of each other. Hence, they define an electric field such that an ionic wind by corona discharge from one electrode is simultaneously created with electrospraying of droplets from the other electrode. Counter ions by the corona discharge interact with the electrosprayed droplets to neutralise the high electric charges, combining forward momentum so that they both move away from the electrodes without the need of external propeller. As stated in several publications [13,28–30], initially highly charge droplets can be neutralized by corona discharge electrode which produces counter ions surrounding the spraying nozzle. In this work, since the pin electrode generating corona discharge acts as the reference electrode for the nozzle generating electrospray, the ion wind impinges and neutralizes the plume of electrosprayed droplets. Our new conceptual design provides a simple but efficient and robust design due to a charge self-balance with simultaneous neutralisation in a free space, generating an low charge aerosol of micro/nano droplet by EHDA. Unlike charged droplets generated by other EHDA systems, uncharged ones exhibit significant improvements in terms of the travelling distance due to not be attracted by charged objects; therefore they will reach their target with much higher efficiency [31].

Figure 1a shows the mechanism of our new EHDA technique comprising one capillary electrode and one pin electrode. Both pin and capillary are placed on the same side, with their tips separate at a distance *d*. When a voltage applied across the two electrodes, an appeared electrical field bends outward due to the discontinuty of the electrical conductivity at the air-liquid surface at the nozzle (Fig. 1b). The accumulated charge causes the liquid surface to protrude out of the capillary and droplets/particles are sprayed from the capillary towards the pin. Simultaneously, the high curvature at the pin tip focuses the electric field outward and nearly parallel to the pin axis [32]. A corona discharge is ignited around the pin

tip and generates a cloud of negative ion wind in parallel with the pin axis *(Figure S1, Supplementary material)*. Under the influence of the electric field, the two clouds of oppositely charged particles by the corona discharge and the electrospraying impinge on each other in the electrode interspace, most of the charge is consumed by ion recombination and bulk flow of charge-reduced particle moves forward and away from both electrodes as propelled by initial momentum from the ionic wind.

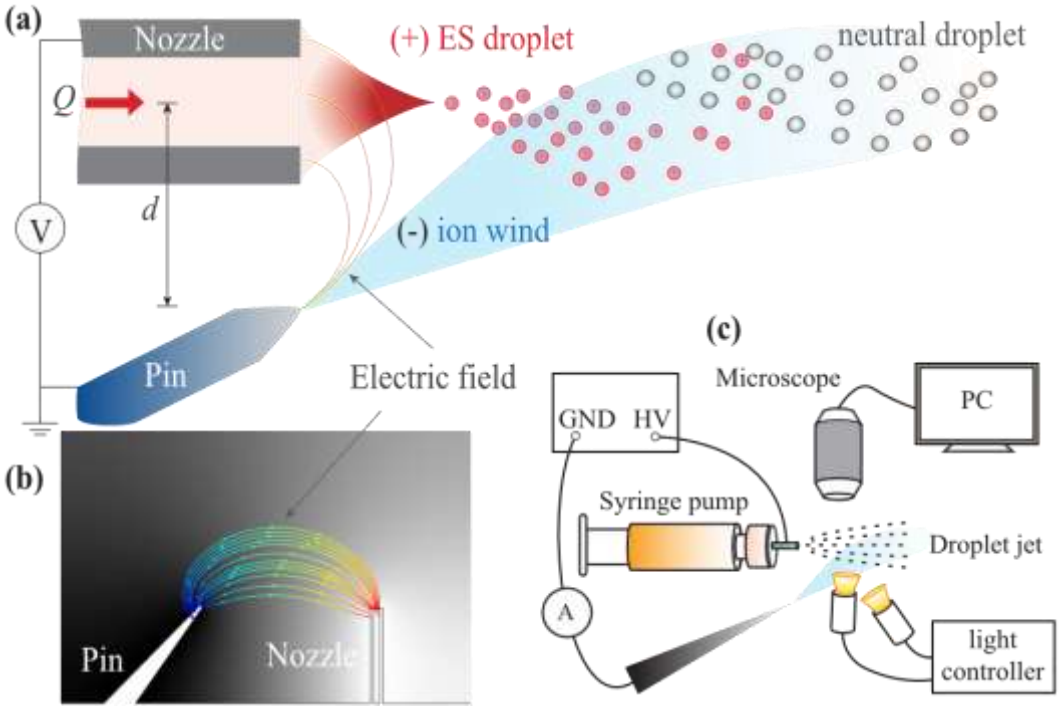

Figure 1 *Mechanism of the present electro-spraying. (a) The generation of a virtual electrode via the space charge effect: the resulting charge reduced droplets form a monodispersed jet; (b) Instantaneous electric field by FEA modeling and (c) Principle schema of the bipolar EHDA experimental apparatus.*

Both electrodes, (i.e. capillary nozzle and pin) are made of stainless steel SUS304. The capillary is a hollow cylinder of 0.2 µm × 0.3 µm (inter diameter × outer diameter). The pin has a diameter of 0.4 mm and is mounted at 50 degree toward the capillary. The pin length is chosen for the ease of system installation. The spherical radius of the pin tip was ~ 40 µm as determined using a microscope. A customised high-voltage generator (+/- 8000V_{pp}) was connected to the electrodes. The discharge current was recorded at the negative electrode. The electrodes were strictly isolated from the stage by polypropylene blocks (with the surface resistivity >10^{16} Ω.sq^{-1}). The experimental data and images were recorded by a digital microscope (i.e. Dino-lite EDGE™). The working liquid was isopropyl alcohol (Sigma-aldrich 99.5%) with the following specifications: surface tension $\gamma \sim$ 20.8 mN/m, density $\rho \sim$ 0.785 g/ml, viscosity $\mu \sim$ 1.66 mPas, conductivity $K \sim$ 6 µS/m and relative permittivity $\varepsilon \sim$ 18.6. The flowrate of injection for a stable Taylor cone is approximated by $Q \sim \gamma\varepsilon\varepsilon_0/\rho K \sim$ 1.59 ml/h (where $\varepsilon_0 \sim$ 5.85 pF/m) and kept at in the range of 0.2 ml/h – 2 ml/h during the experiment by a syringe pump (NE-1000). The main reason for the choice of pure fluids with low surface tension instead of using surfactant

solutions is to exclude the surface tension variation of the liquid due to nonuniform distribution of the surfactant molecules by a focused electric.

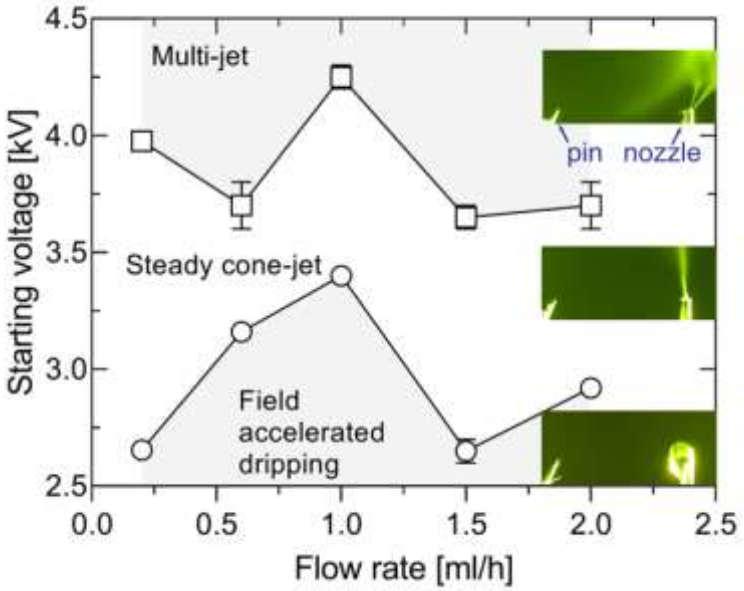

Figure 2 *Staring voltage plotted versus flowrate by the present EHDA electro-spraying of isopropanol alcohol for the 3 modes: (i) Upper voltage boundary is observed between multi-jet discharge and steady Taylor cone jet regime; (ii) Lower voltage boundary is determined between the steady Taylor cone jet and field accelerated regime and (iii) Steady Taylor cone formation and jet stream are observed at a relatively broad range of voltages and flow rates.*

Figure 2 shows the voltage-flowrate diagram for the three different phases including the field accelerated dripping, the steady Taylor cone-jet, and the multi-jets. At a given flowrate, a voltage range for the steady Taylor cone phase is confined between two limits: the upper voltage for the multi-jet phase and the lower one for the dripping phase. Experimental results show that the formation of the steady Taylor cone has achieved at a broad range of voltages. For instance, the steady Taylor cone-jet was observed across a flowrate 0.2 ml/h with a range of voltages from 2.65 kV – 3.97 kV. Furthermore, corona discharge and ionic wind were observed at the pin electrode while the spraying capillary plays the role of a reference electrode (Fig. 2 - inset).

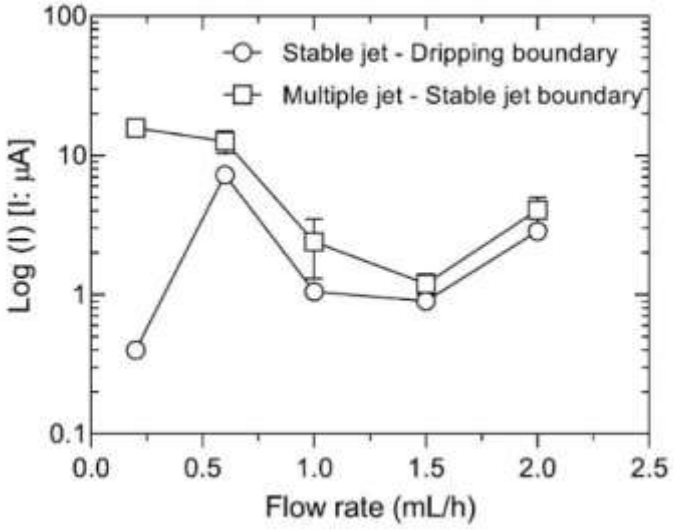

Figure 3 *Current plotted vs Flowrate by the present EHDA spraying of isopropanol alcohol for the 3 modes: (i) Upper voltage boundary between multi-jet discharge and steady Taylor cone jet regime; (ii) Lower voltage boundary between the steady Taylor cone jet and field accelerated regime and (iii) Steady Taylor cone formation and jet stream are observed at a broad range of voltages and flow rates.*

Figure 3 presents the relationship between the current and flow rate to achieve a stable spraying. Compared with the voltage, a much wider range of current is associated with stable electrospraying. By the experiment, the stable Taylor cone can be observed at a relatively small current, e.g. 0.4 μA at a flowrate of 0.2 ml/h and increasing to 14.7 μA at the multi jet mode. It is well-known that the current of the electrospray is much lower than 1 μA [33], thus most of charges are for the corona discharge but not the electrospray. This uniquely wide range of discharging current allows a practical approach to keep the spray process stable and prevent the electrodes from degradation by simply controlling the discharge current of the system via a feedback loop [34]. Furthermore, the V-I characteristic of the system aligns with that of the bipolar discharge, as the relation $\log(I) \propto \log(V - V_0)$ fit better than the empirical Townsend relationship $I/V \propto V$[35]. We noted that the starting current significantly varies with different flowrates a slightly higher voltage is required for a higher flowrate *(Figure S2, Supplementary material)*

For a discharge currents (I) greater than 1 μA, the corresponding ion wind flow can be estimated by $U = k\sqrt{I/\rho\mu}$; where k (~ 0.003 m^{-1}) is a constant and depends on the electrode discharge area and the inter-electrode distance d (d = 5 mm in this work), $\mu = 1.6 \times 10^{-4}\ m^2 \cdot V^{-1} \cdot s^{-1}$ the mobility of positive and negative charges, $\rho = 1.204\ kg \cdot m^{-3}$ the air density [3637]. The ion wind from pin electrode can reach an average velocity of 0.83 m/s at a discharge current of 14.7 μA and can control the spray direction of the spray angle θ of droplet cloud from nozzle electrode.

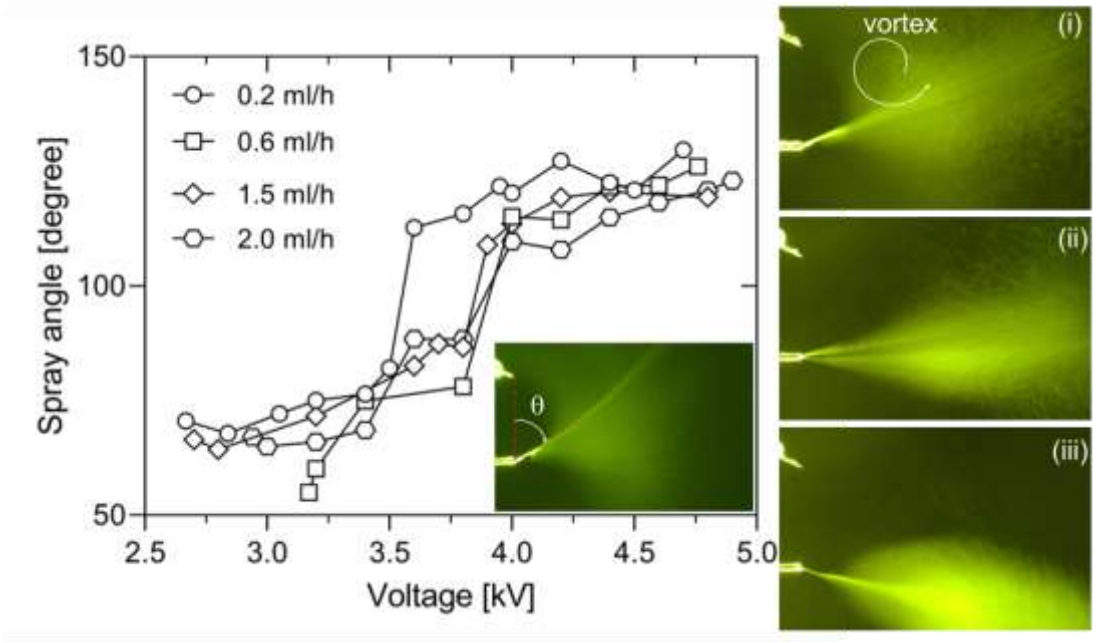

Figure 4. *Relationship of the direction between the praying jet stream (by angle θ) and the driving voltage of the present EHDA method for several flowrates: 0.2, 0.6, 1.5 and 2.0 ml/h. Optical images of the jet stream for 3 different DC sources: (i) 3.66kV-1.1μA: particles/droplets fly back to the pin electrode while part of them being propelled away by the ion wind, as observed by a visible vortex in inset i; (ii) 4.0kV-1.7μA: particles move away from capillary as observed in inset ii and (iii) 4.25kV-15μA jet stream of sprayed droplets was further deflected due to stronger ionic wind. Pin and capillary tip can be seen at the left side of insets (distance between the pin and capillary tip is 5 mm, spray rate is 1ml/h)*

The angle θ shown in the left inset of Fig. 4 indicates the direction of the particles' trajectory when they move out the capillary. Once generated from the capillary tip, the sprayed particles divert towards the pin electrode while being neutralized and propelled by the ionic wind. Experimental results depict the impact of the driving voltage on the direction of the sprayed jet stream. At a relatively low voltage of 3.66 kV, under the impingement of ion wind, a cloud of generated particles moves along a trajectory of $\theta \sim 52°$ forward to the pin electrode and create a visible vortex as shown in Fig. 4(i). A number of particles can reach and wet the pin. As the driving voltage increases then the ion wind is increasingly strong until achieves sufficient momentum to propel the flow of sprayed particles away the electrodes. When the driving voltage reaches 4.0kV, the stream of particles moves forward with $\theta \sim 83°$ (see Fig. 4(ii)). A much stronger ion wind (for example at a voltage of 4.25 kV) can even push the Taylor cone outward ($\theta \sim 105°$) and the spray plume visually expands downstream (see Fig. 4 (iii)). This forwarding movement indicates that the net charge is reduced and electrostatic force has been dramatically mitigated. Remarkably, experimental observations show that the spraying direction is stable while the pin electrode does not attract any visible particles.

It is worth noting that the curvature of pin tip plays an important role in defining the discharge current for the electrospraying. A pin of larger tip (sphere radius 300 μm) requires a much higher threshold voltage for corona discharge and is not be able to generate sufficient ion wind, and thus most of sprayed

particles will move toward the pin electrode, yielding a destabilisation of the spraying process *(Figure S3, Supplementary material)*

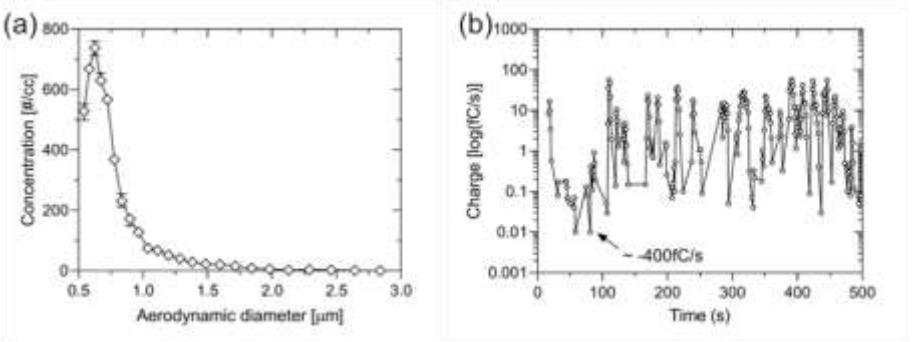

Figure 5. *Experimental results: (a) Particle size distribution, plotted vs liquid concentration, covers a range of 500nm to 2000 nm and (b) Measured particle charge at the downstream vs. time at a voltage of 4 kV and current of 1.7 μA.*

Finally, Figure 5(a) shows the particle size distributions measured using aerosol spectrometer (TSI 3340) placed at downstream at a distance of 100 mm from the capillary tip as shown in Fig. 1(c). The system is powered with 4kV-1.7μA. A high concentration of particle sizes ranging 0.5 μm-1.5 μm is recorded, which is larger than the charged particles that were passing through the charge diffusion of a typical electrospray process [38]. This proved that the generated nanoparticles are efficiently charge reduced and delivered. In addition, results in Fig. 5(b) measured by an electrometer probe (TSI 3608) show that the charge of particle cloud is in order of tens of fC/s (i.e. fA), with a start-up value of -400 fC/s. The start-up charge is corresponding to the initial turbulence caused by the corona discharge and electrospraying and reflects the interaction between negative and positive particles of the present method, which then result in an extremely low charge level compared with the total spray current of 1.7 μA, and is one thousand times smaller than reported mean droplet charge by electrospray [39]

In conclusion, we present a versatile EHDA based system using a capillary nozzle and pin configuration powered by DC voltage without the need of collector electrode which is essential in most existing EHDA systems for forward delivery of aerosols. The new system generates particles/droplets and delivers them in the form of a continuous and stable jet stream of charge reduced micro/nano particles. This unique advantage would enable the present system to efficiently deliver drug nanoparticles in biomedical and nanomedicine applications.

Supplementary material: See the supplementary material for corona discharge, analysis of I-V characteristics, and effect of the curvature of pin tip.

Data Availability: The data that supports the findings of this study are available within the article and its supplementary material.

References

[1] M. Nikolaou and C.T. Krasia, Eur. J. Pharm. Sci. **113**, 29 (2018).
[2] A. Pawar, S. Thakkar, and M. Misra, J. Control. Release **286**, 179 (2018).
[3] P. Zanen, L.T. Go, and J.W.J. Lammers, Int. J. Pharm. **114**, 111 (1995).
[4] M.J. Telko and A.J. Hickey, Respir. Care **50**, 1209 (2005).
[5] S.A. Hofstadler and K.A. Sannes-Lowery, Nat. Rev. Drug Discov. **5**, 585 (2006).
[6] M. Wleklinski, B.P. Loren, C.R. Ferreira, Z. Jaman, L. Avramova, T.J.P. Sobreira, D.H. Thompson, and R.G. Cooks, Chem. Sci. **9**, 1647 (2018).
[7] Q.T. Zhou, P. Tang, S.S.Y. Leung, J.G.Y. Chan, and H.K. Chan, Adv. Drug Deliv. Rev. **75**, 3 (2014).
[8] M.B. Dolovich and R. Dhand, Lancet **377**, 1032 (2011).
[9] J.-W. Yoo, D.J. Irvine, D.E. Discher, and S. Mitragotr, Nat. Rev. Drug Discov. **10**, 521 (2011).
[10] J. Zeleny, Phys. Rev. **10**, 1 (1917).
[11] J.C. Ijsebaert, K.B. Geerse, J.C.M. Marijnissen, J.W.J. Lammers, and P. Zanen, J. Appl. Physiol. **91**, 2735 (2001).
[12] A. Jaworek, A.T. Sobczyk, and A. Krupa, J. Aerosol Sci. **125**, 57 (2018).
[13] G.M.H. Meesters, P.H.W. Vercoulen, J.C.M. Marijnissen, and B. Scarlett, J. Aerosol Sci. **23**, 37 (1992).
[14] T. Ciach, Int. J. Pharm. **324**, 51 (2006).
[15] J.P. Borra, D. Camelot, K.L. Chou, P.J. Kooyman, J.C.M. Marijnissen, and B. Scarlett, J. Aerosol Sci. **30**, 945 (1999).
[16] J.C. Almekinders and C. Jones, J. Aerosol Sci. **30**, 969 (1999).
[17] J. Fernandez de la Mora and C. Barrios-Collado, Aerosol Sci. Technol. **51**, 778 (2017).
[18] J.P. Borra, D. Camelot, J.C.M. Marijnissen, and B. Scarlett, J. Electrostat. **40**–**41**, 633 (1997).
[19] V.T. Dau and T. Terebessy, US patent No. US9937508 (February 2014).
[20] V.N. Morozov, J. Aerosol Sci. **42**, 341 (2011).
[21] F. Mou, C. Chen, J. Guan, D.-R. Chen, and H. Jing, Nanoscale **5**, 2055 (2013).
[22] L.Y. Yeo, D. Lastochkin, S.C. Wang, and H.C. Chang, Phys. Rev. Lett. **92**, 2 (2004).
[23] P. Wang, S. Maheshwari, and H.C. Chang, Phys. Rev. Lett. **96**, 3 (2006).
[24] N. Chetwani, S. Maheshwari, and H.C. Chang, Phys. Rev. Lett. **101**, 1 (2008).
[25] N. Chetwani, C.A. Cassou, D.B. Go, and H.C. Chang, J. Am. Soc. Mass Spectrom. **21**, 1852 (2010).
[26] D.B. Bober and C.-H. Chen, J. Fluid Mech. **689**, 552 (2011).
[27] V.T. Dau, T.-K. Nguyen, and D.V. Dao, Appl. Phys. Lett. **116**, 023703 (2020).
[28] K. Tang and A. Gomez, J. Aerosol Sci. **25**, 1237 (1994).
[29] J.F. de la Mora and A. Gomez, J. Aerosol Sci. **24**, 691 (1993).
[30] V.T. Dau, T.X. Dinh, C.-D. Tran, T. Terebessy, T.C. Duc, and T.T. Bui, J. Aerosol Sci. **124**, 83 (2018).
[31] I.M. El-Sherbiny, N.M. El-Baz, and M.H. Yacoub, Glob. Cardiol. Sci. Pract. **2015**, 2 (2015).
[32] V.T. Dau, T.X. Dinh, T.T. Bui, C.D. Tran, H.T. Phan, and T. Terebessy, Exp. Therm. Fluid Sci. **79**, 52 (2016).
[33] M. Drotboom, H. Fichtner, and H. Fissan, J. Aerosol Sci. **28**, 535 (1997).
[34] V.T. Dau, T.T. Bui, T.X. Dinh, and T. Terebessy, Sensors Actuators A Phys. **237**, 81 (2016).
[35] V.T. Dau, C.D. Tran, T.X. Dinh, L.B. Dang, T. Terebessy, and T.T. Bui, IEEE Trans. Dielectr. Electr. Insul. **25**, 900 (2018).
[36] V.T. Dau, T.X. Dinh, T. Terebessy, and T.T. Bui, IEEE Trans. Plasma Sci. **44**, 2979 (2016).
[37] L. Li, S.J. Lee, W. Kim, and D. Kim, J. Electrostat. **73**, 125 (2015).
[38] J. Xie, J. Jiang, P. Davoodi, M.P. Srinivasan, and C.H. Wang, Chem. Eng. Sci. **125**, 32 (2015).
[39] A. Jaworek and A. Krupa, in *Sprays Types, Technol. Model.* (Nova Science Publishers, 2011), pp. 1–100.